[redacted]
ELSEVIER
Ultrasonics 36 (1998) 883–892

[redacted]

Dan Phillips *, Xucai Chen, Raymond Baggs, Deborah Rubens, Michael Violante,
Kevin J. Parker

Rochester Center for Biomedical Ultrasound, University of Rochester, Rochester, NY 14627, USA

[redacted]

Abstract

[redacted] enhancement capabilities. The durability of these bubbles in the blood stream has been found to be limited, providing impetus for a number of approaches to further stabilize them. One of the approaches has been the development of micrometer-size porous [redacted] morphology and surface chemistry involved in the production of this type of agent makes it unfeasible to directly measure the [redacted] fraction of gas should be necessary to significantly enhance the echogenicity of this type of particle-based contrast agent. In the [redacted] scatterer and the overall scatterer diameter. Initially, the volume fraction of gas is considered as a discrete entity or single bubble. Using common mixture rules, it is then shown that the gas can be considered to be distributed throughout the particle and still arrive at a result that is similar to that for a single, discrete volume of gas. The main contribution to the increased scattering cross-section is due to the compressibility difference between gas and water. The backscatter coefficient is computed as the product [redacted]

Keywords: Ultrasound; Contrast; Bubble

1. Introduction

Diagnostic ultrasound images are formed from the acoustic pressure waves reflected from various scattering tissues and structures within the body. The image bright- [redacted] location, relative acoustic properties, and the frequency, [redacted]

Two of the acoustic properties which determine the scattering strength of a structure are its density, ρ, and [redacted]

enhanced backscatter contrast provided by the particle/bubble agent.

The use of air and other gases for ultrasound contrast enhancement has a long history. An early study involved the injection of small air bubbles into the blood [1]. [redacted] persed, they are eliminated in the pulmonary capillary bed, where they are trapped and gradually absorbed. Additionally, the high pressure experienced in the left [redacted] that manage to pass through the pulmonary circulation. Unfortunately, these elimination mechanisms rule out acoustic contrast enhancement for a majority of soft tissues using intravenous injection of free bubbles.

* Corresponding author. Tel.: (716) 275 4066/(716) 275 9542; fax: (716) 473 0486; e-mail: phillips@ee.rochester.edu

[redacted]

smaller than a red blood cell are less apt to produce a harmful obstruction to flow within a capillary bed. An additional benefit of small bubbles with diameters less than 10 μm is that their acoustic resonance peaks lie [redacted] account, Miller [3] derived an expression for the resonance frequency, f_0, of a free bubble as

$$f_0 = \frac{1}{2\pi a}\sqrt{\frac{3\gamma}{\rho}\left(p_0 + \frac{2\sigma}{a}\right) - \frac{2\sigma}{a\rho}} \quad (1)$$

where γ is the ratio of heat capacities of the gas at constant pressure and volume, a is the radius of the bubble, p_0 is the ambient pressure and ρ is the density of the surrounding medium. Using this expression for a free air bubble in water, the resonance frequency is 11.9 MHz when $a = 0.5$ μm and 4.86 MHz when $a = 1$ μm. This resonance in the oscillatory behaviour of a bubble serves to enhance the acoustic scattering cross-section (to be discussed later) of the bubble as shown in Fig. 1.

However, it would appear that nature conspires to eliminate small bubbles. Surface tension acts to eliminate free bubbles as their radius decreases [4,5]. The pressure due to surface tension (p_{st}) exerted on the gas inside a bubble is [5] $p_{st} = 4\sigma/a$. Based on diffusion and surface tension alone, it has been estimated that a bubble with a radius of 10 μm would completely collapse in less than [redacted] Given the complex chemical environment of the blood,

In an attempt to capitalize on the inherent contrast enhancing effect of a gas bubble, a number of strategies have been pursued which could ultimately result in its use as a safe, stable, consistent and possibly quantifiable [redacted] which consists of a suspension of stable, gas-bearing particles. It should be noted that a suspension refers a mixture of a fluid and defined concentration of insoluble objects that are dispersed in the fluid. These suspensions provide increased ultrasound contrast when imaging the liver, and have the potential for providing similar blood pool enhancement for Doppler flow studies. The particles are relatively dense, solid spheres, 1–2 μm in diameter, whose preparation results in a complex surface morphology and surface chemistry that facilitates the entrapment and stabilization of air bubbles on or within ~~the particle. An earlier X-ray and ultrasound contrast~~ agent consisting of solid spheres comprised of IDE (iodapamide ethyl ester) [12,13] is shown in Fig. 2(a). A particle/bubble agent, 'Bubbicles', shown in Fig. 2(b), is also comprised of IDE. Its manufacture produces an irregular surface morphology that provides numerous hydrophobic crevices suitable for the stabilization of gas bubbles. This agent is delivered into the blood stream as a suspension with sufficient concentration to enhance the ultrasonic contrast between the plasma it is carried in and the tissues to which it is delivered. The Kuppfer [redacted] majority of the delivered dose after 10–20 min. This

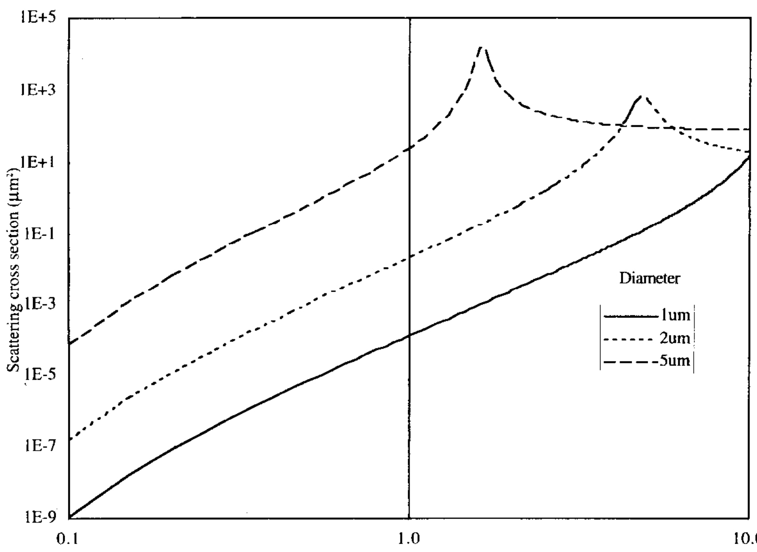

Fig. 1. Backscatter cross-sections (μm²) for an air bubble in water. Parameters used for calculation: $\rho = 998$ kg m^{-3} (water), $\sigma = 7.305 \times 10^{-2}$ N m^{-1} (air/water interface), $\gamma = 1.402$ (ratio of specific heats, adiabatic), $p_0 = 1.013 \times 10^5$ Pa (ambient pressure, 1 atmosphere).

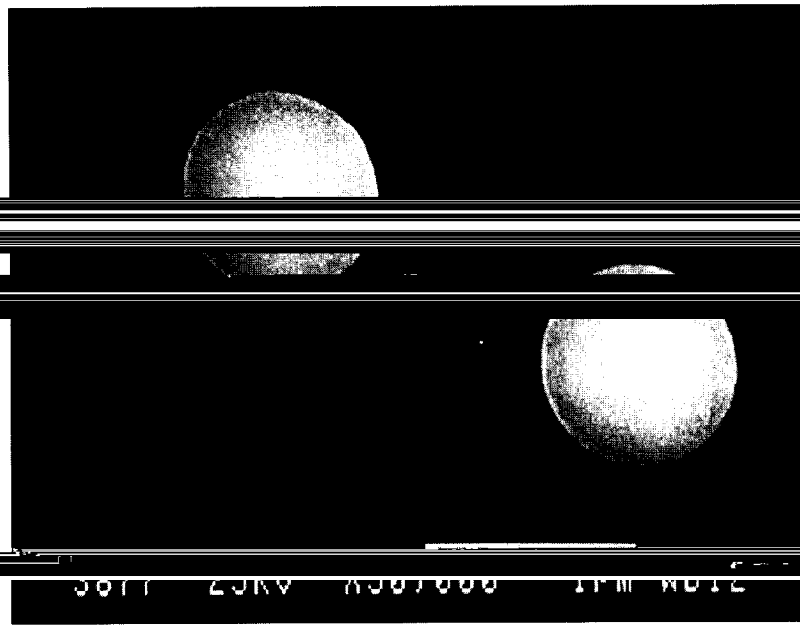

(a)

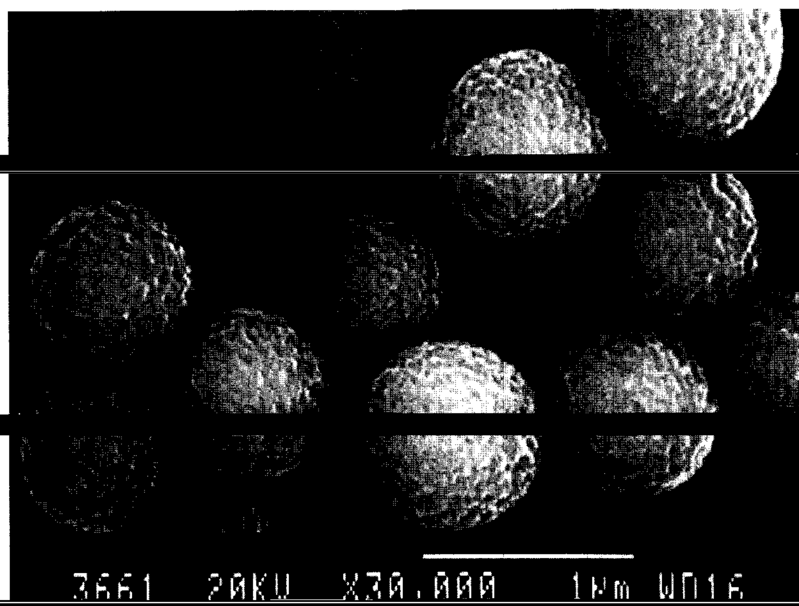

(b)

results in a phase of blood pool enhancement on the order of ten minutes which is followed by a period of liver enhancement [14,15].

It should be noted that the actual size distribution of both the IDE spheres and the particle/bubble agent ('Bubbicles') results in a lognormal distribution with a standard deviation that is typically one-third of the mean measured diameter of the scatterers. More importantly, the mean value for the size distribution can be tightly controlled and is highly repeatable (± 50 nm for a specified diameter of 1 μm). For the purposes of this discussion, we will consider suspensions or either IDE or 'Bubbicles' with a uniform size distribution and a constant number density (number of scatterers per unit volume) that corresponds to a concentration of 10 mg of either 1 or 2 μm diameter solid IDE particles in a 1 ml volume of water. This will help focus our investigation of the small amount of entrained gas that needs to be stabilized within the rough, irregular surface and spatial structure of the particle/bubble agent to significantly enhance its echogenicity. The effects of a non- [illegible] will be addressed in the discussion.

2. Theoretical model of the particle/bubble agent

There are three scattering regimes which may be characterized by the relative size of the scattering object compared to the wave length of the incident acoustic wave. The product ka (where $k=2\pi/\lambda$ is the wavenumber [illegible] differentiate these regimes, which correspond to the cases where $ka \gg 1$, $ka \approx 1$ and $ka \ll 1$. We will be interested in the situation where $ka \ll 1$ (the scatterers are much smaller than the wavelength of the incident wave) [illegible] can be described by a distribution function which tends [illegible] smaller.

If we assume a speed of sound in water of 1490 m s^{-1}, then for an insonifying frequency of 5 MHz, [illegible] of 1 μm ($a=0.5$ μm) and $ka=2.12\times10^{-2}$ for a diameter of 2 μm ($a=1$ μm). For a 1 μm diameter free bubble at resonance ($f_0=11.9$ MHz) $ka=2.53\times10^{-2}$; for a 2 μm diameter free bubble at resonance ($f_0=4.86$ MHz) $ka=2.07\times10^{-2}$. In both cases, k, the wave number, assumes propagation in water. Therefore the only situations in which resonance effects would come [illegible] fraction of gas in the particle/bubble agent is close to unity (i.e., close to being totally comprised of gas). As resonance effects would serve to augment the backscatter coefficient, the proposed model may slightly underestimate the scattering of particle/bubble agent for the larger 2 μm scatterers that are comprised almost completely of gas. In the case of the particle/bubble agent, [illegible] gas is so small as to be visually indistinguishable by light microscopy. [illegible] agent does not exhibit buoyant behaviour, the volume of entrapped gas is less than 58% of the particle/bubble combination. This is based on a simple calculation involving the density of the IDE material that the particle/bubble agent is comprised of and that of the [illegible]

To indicate the scattering efficacy of the [illegible] single particle/bubble pair will be considered initially. This is defined as the amount of energy re-directed from [illegible] of the incident wave, the result having the units of area [16].

The scattered acoustic pressure, p_s, at a distance r from a sphere with compressibility κ_e and density ρ_e embedded in a medium with compressibility κ and density ρ when $ka \ll 1$, is given [16] by

$$p_s(r,\varphi)=A\frac{e^{ikr}}{r}\Phi(\varphi) \tag{2}$$

[illegible] is the scattering angle (π for backscatter) and

$$\Phi(\varphi)=\frac{1}{3}k^2a^3\left(\frac{\kappa_e-\kappa}{\kappa}+\frac{3\rho_e-3\rho}{2\rho_e+\rho}\cos\varphi\right). \tag{3}$$

[illegible]

$$\sigma_d=|\Phi(\varphi)|^2. \tag{4}$$

A parameter that will allow comparison of the efficacy of the scattering of our models with physiological tissue, such as liver and blood, is the backscatter coefficient, [illegible] steradians). For a distribution of discrete scatterers, the backscatter coefficient is found to be equal to the mean backscatter cross-section per unit volume, in other words,

$$\eta_{BS}=n\sigma_d(\pi) \tag{5}$$

where n is the number density of the scatterers. The [illegible] amount of backscattered power from a number of identical scatterers in a given volume that are exposed to the same incident pressure wave. Since direct evaluation of this value for a soft tissue requires knowledge of the scattering structures, their characteristics and number density within the tissue, these values are arrived at experimentally by measurement, comparison and [illegible] values reported in the literature for η_{BS} are given in Table 1.

It is essential to acknowledge that the following models incorporate only gross physical characteristics and features of the agent involved. They do not address [illegible] ment of echogenicity of the particle/bubble agent with [illegible] fraction of gas and guide further development and

Table 1
η_{BS} values

Substance	η_{BS} ($m^{-1}\ sr^{-1}$)	Source
Liver		
Standard	3.0×10^{-1}	AIUIM [23]
Average	1.9×10^{-1}	Nassiri and Hill [24]
[redacted]		
Tumor	1.4×10^{-1}	Nassiri and Hill [24]
Fixed	1.9×10^{-1}	Nassiri and Hill [24]
Bovine	1.76×10^{-1}	Fei and Shunt [25]
Blood		
26% HMTC	2.8×10^{-3}	Nassiri and Hill [24]
[redacted]		
40% HMTC	7.7×10^{-3}	Nassiri and Hill [24]
40% HMTC	6.9×10^{-3}	Shung et al. [26]

optimization of this agent. Part of the incentive for developing this model stems from the fact that it was not feasible to directly ascertain through laboratory measurements the volume of gas entrapped in the [redacted] surface chemistry and morphology.

The modeling incorporates the concept of an effective scatterer of radius a containing some volume fraction of gas. Parameters used to describe this effective scatterer are a_p (the radius of a sphere containing the equivalent volume of solid material in the scatterer), a_g (the radius of a sphere containing the equivalent volume of gas in the scatterer), a (the overall radius of the scatterer) and x (the volume fraction of gas in the scatterer). The relationship between these four parameters is

$$a_p^3 = a^3(1-x), \quad a_g^3 = a^3 x. \tag{6}$$

3. Modeling

One way to model the scattering behaviour of the [redacted] located next to a solid particle with a radius such that the volume of the single bubble plus the volume of the idealized solid particle equals the volume of the actual particle/bubble agent under consideration (Fig. 3(B)). [redacted] there is a negligible phase difference). The bubble and [redacted] in the particle/bubble pair.

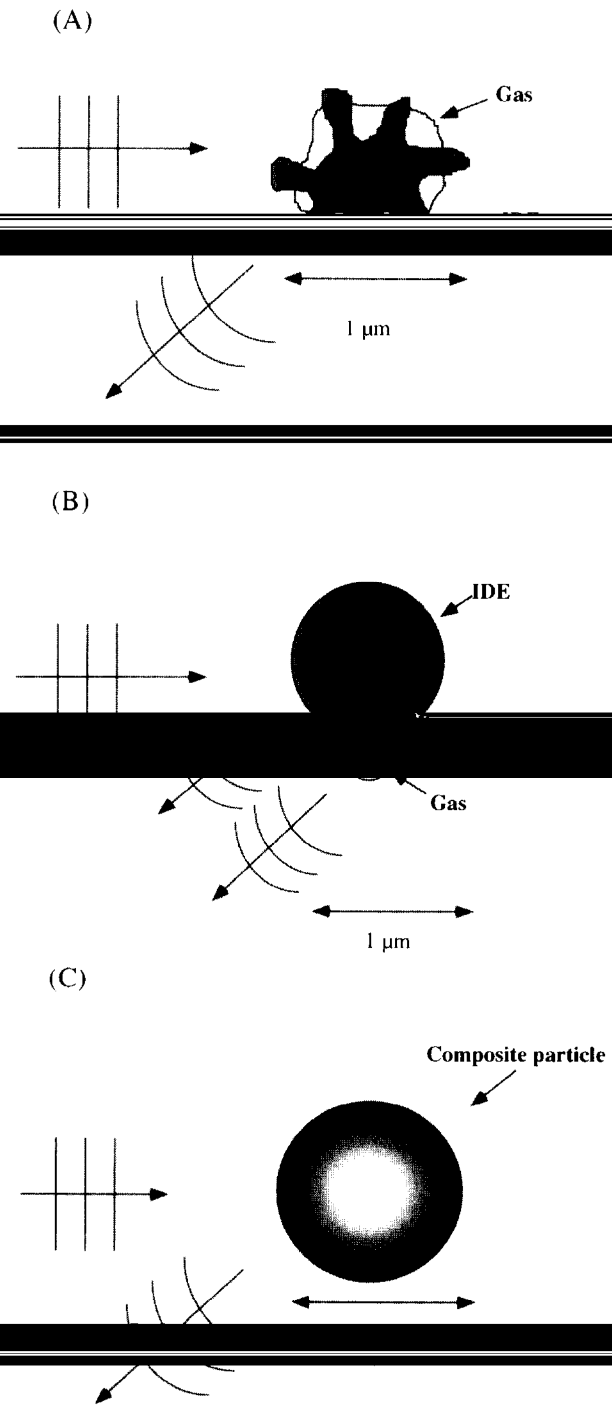

Fig. 3. Schematic representation of the model. (A) The actual particle/bubble pair; (B) Approach 1: coherent summation of two inde- [redacted]

[redacted] volume of gas is sub-divided into multiple, smaller [redacted] into a single, larger scattering volume.

For the coherent scattering of the particle/bubble pair [redacted] tion of the pair Φ_t is the sum of scattering angle distribution function of the bubble, Φ_g and the scattering angle distribution function of the particle, Φ_p.

$$\Phi_t(\varphi)=\Phi_g(\varphi)+\Phi_p(\varphi). \tag{7}$$

Given that the particle material has compressibility κ_p and density ρ_p and the gas being discussed has compressibility κ_g and density ρ_g, we can define the [redacted] of the particle and gas with respect to water as γ_{ρ_p} and γ_{ρ_g}. We define the compressibility difference between a scattering material s and the propagating medium m (in this case water) as

$$\gamma_{\kappa_s}=\frac{\kappa_s-\kappa_m}{\kappa_m} \tag{8}$$

and the analogous density difference as

$$\gamma_{\rho_s}=\frac{3\rho_s-3\rho_m}{2\rho_s+\rho_m}. \tag{9}$$

A simple substitution of Eq. (3) for the bubble and the particle into Eq. (7), combined with the relationships in Eq. (6), results in the following expression:

$$\Phi_t(\varphi)=\tfrac{1}{3}k^2a^3[x(\gamma_{\kappa_g}+\gamma_{\rho_g}\cos\varphi)$$

[redacted]

Utilizing Eq. (10), we can evaluate Eq. (4) for $\varphi=\pi$, arriving at an expression for the differential backscattering cross-section for the particle/bubble pair

[redacted]

An alternative way to model the particle/bubble agent is to combine the scattering behaviour of particle and gas components into an 'equivalent scatterer' with a specified volume fraction of gas.

[redacted] expressed [18] as

$$\kappa_e=(1-x)\,\kappa_p+x\kappa_g. \tag{12}$$

[redacted] and ρ_p (particle), a similar linear mixing relationship for the effective density can be derived, where the effective density, ρ_e, is shown to be

$$\rho_e=(1-x)\,\rho_p+x\rho_g. \tag{13}$$

Thus, we can model the complex particle/bubble [redacted] terer with some effective density and compressibility, as [redacted] ρ_e for κ_s and ρ_s in Eqs. (8) and (9) and then substituting the resultant expressions in Eqs. (8) and (9) into Eqs. (3) and (4) results in a differential backscattering cross-section where

$$\sigma_d(\varphi=\pi)=|\Phi(\varphi=\pi)|^2=\tfrac{1}{9}k^4a^6|\gamma_{\kappa_e}^2-2\gamma_{\kappa_e}\gamma_{\rho_e}+\gamma_{\rho_e}^2|. \tag{14}$$

The equivalence of the two formulations of the model is exhibited in Fig. 4, which shows the backscatter [redacted] solid IDE particles alone (no gas) calculated using both approaches, for particle/bubble scatterers with overall diameters of 1 and 2 μm. This concentration produces a number density, n, of 7.94×10^{12} particles m^{-3} for 1 μm diameter solid IDE spheres and 9.90×10^{11} particles m^{-3} for 2 μm diameter solid IDE spheres; these numbers were held constant in the calculations. The only region of the graph which exhibits any distinguishable difference between the two modeling approaches is in the extreme case corresponding to a volume fraction of gas equal to one, which essentially describes a simple gas bubble. The two models give very similar results for the size and frequency considered. It is also observed from Fig. 4 that there is a relatively constant, low backscatter coefficient for volume fractions of gas below 1×10^{-4} which then increases exponentially as the [redacted]

4. Experimental evaluation

[redacted] by individual particles of the agent or to modulate it to any specified level, scattering measurements were taken of 'Bubbicles' suspensions and suspensions of plain IDE spheres with the same concentration and particle size [redacted] maximum volume fraction of air was assumed to be [redacted] to make the 'Bubbicles' neutrally buoyant.

[redacted] utilizing a method similar to Wear [19] except for the use of a tone burst excitation signal with a frequency of 5 MHz. The use of a tone burst insonification helped provide signals with an increased signal to noise ratio and simplified the measurements. Calibration of the measurement system was based on methods described [redacted]

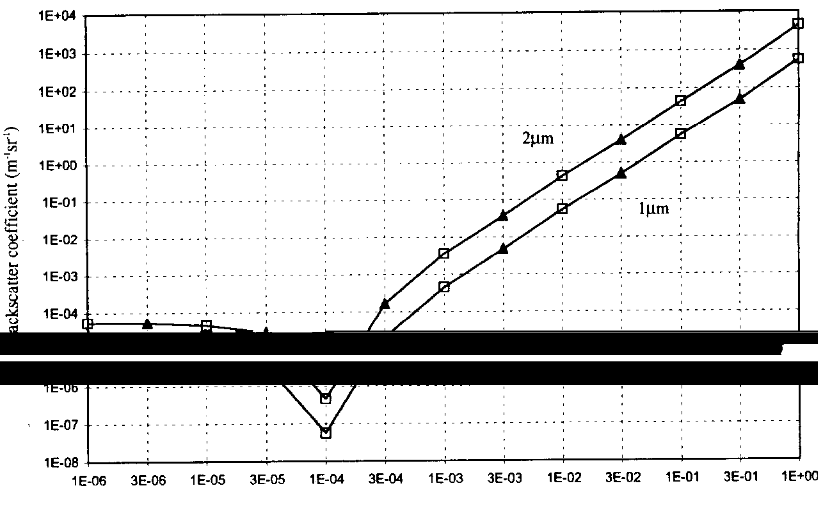

Fig. 4. Backscatter coefficient at 5 MHz calculated from both models as functions of volume fraction of gas, x. Since results from Model 1 (solid triangles) and Model 2 (open squares) were similar, alternate values of each curve are displayed. The suspension medium is water, and the gas in the agent is air. The concentration of the agent is $10\ \mathrm{mg\ ml^{-1}}$. Parameters used: water $\kappa_{H_2O}=4.6\times10^{-10}\ \mathrm{m^2\ N^{-1}}$, $\rho_{H_2O}=998\ \mathrm{kg\ m^{-3}}$, $c_{H_2O}=1.48\times10^3\ \mathrm{m\ s^{-1}}$, air $\kappa_g=7.0\times10^{-6}\ \mathrm{m^2\ N^{-1}}$, $\rho_g=1.29\ \mathrm{kg\ m^{-3}}$, solid IDE $\kappa_p=2.0\times10^{-11}\ \mathrm{m^2\ N^{-1}}$, $\rho_p=2.40\times10^3\ \mathrm{kg\ m^{-3}}$.

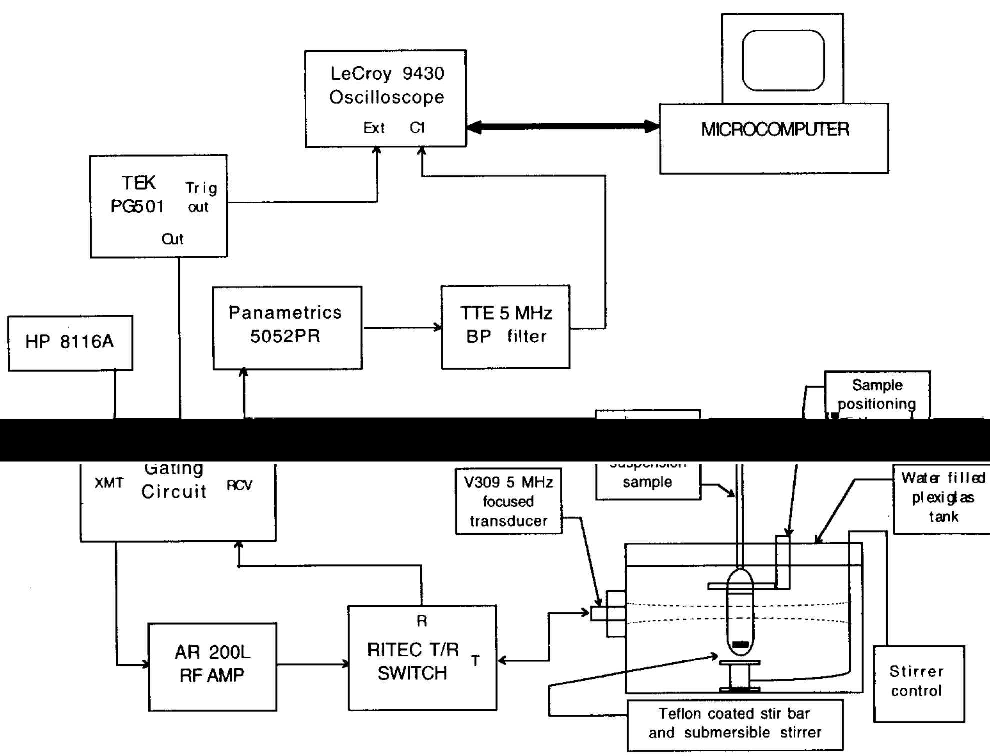

Fig. 5. Block diagram of equipment configuration for experimental measurements. See text for details.

modification for the use of a focused transducer based on the diffraction correction formulation of Chen [22]. A system backscatter coefficient calibration factor was [illegible] of the transducer allowed evaluation of the measurement [illegible]

ral of the radiation pattern and use of a diffraction correction factor.

Measurements were carried out with a gated transmis- [illegible] The 10 cycle, 5 MHz tone burst was generated by a [illegible] being amplified by an Amplifier Research AR200L radio frequency (RF) amplifier. The output of the RF amplifier was routed to a Panametrics V309 narrow band, 6.35 mm radius transducer focused at 56.9 mm through a RITEC transmit/receive (T/R) switch. The suspension samples were contained in an acoustically transparent [redacted] water. The suspension was slowly and continuously [redacted] bottom of the sample pipette which was rotated by a [redacted]

The received signal was gated for a 10 μs epoch centered at the focal distance of the transducer to avoid specular reflections from the wall of the pipette and then [redacted] gated Panametrics 5052PR pulser/receiver, filtered by a [redacted] by a LeCroy 9430 high speed digital oscilloscope. Each measurement consisted of 50 sequential 10 μs scans sampled at a rate of 100 MHz that were stored in the oscilloscope and then downloaded via an IEEE-488 parallel bus connection to an IBM-PC compatible microcomputer running custom written programs utilizing the ASYST software package. Each 10 μs scan consisted of [redacted] lated by taking the mean of the measured power at 5 MHz and dividing it by a calibration factor that accounts for the electromechanical response of the system. The calibration factor was derived from the measurement of the system response to the reflection from a flat Panametrics stainless steel calibration block placed at the transducer focus and incorporates a diffraction correction factor for the beam pattern of a [redacted] of the bar chart in Fig. 6 which shows measured back- [redacted] (not expected to stabilize gas) and representative values [redacted] suspension of 'Bubbicles' has an effective volume fraction of gas of 3%. This corresponds to a volume fraction of 3×10^{-2} in Fig. 4 (a volume 1.57×10^{-20} m^3 relative [redacted] 5.24×10^{-19} m^3 or a volume of 1.26×10^{-19} m^3 relative [redacted] 4.19×10^{-18} m^3). Even at this minute volume fraction, the backscatter coefficient of the suspension is comparable with or higher than the representative values for liver given in Table 1.

5. Discussion

[redacted] of results from two approaches to the model stems from the fact that both approaches incorporate a linear

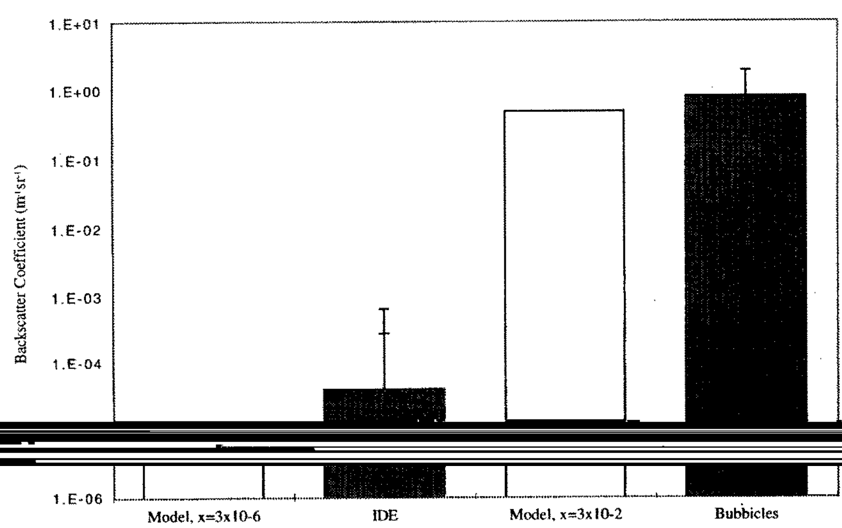

Fig. 6. Comparison of model predictions with experimental data at 5 MHz. The error bars represent the absolute value of the backscatter coefficient obtained due to plus or minus one standard deviation of the measured power scattered from the samples. Mean and standard deviation of the measured backscattered power were obtained from a series of 50 consecutive radio frequency waveforms.

dependence on the volume fraction of stabilized gas, and furthermore that the gas compressibility and density dominate the scattering process.

The scattering model predicts that only small gas [redacted] regions in blood and less than 10% for liver at concen- [redacted] distinction when compared with the majority of contrast agents currently available, which typically consist of a gas filled region with a thin shell or coating for stabiliza- [redacted] with a volume fraction of gas close to 1, that is, nearly 100% of the total scatterer volume.

[redacted] particles is slightly lower than the measured result. This could be partly due to the fact that the measured IDE particles have some percentage of diameters above and below 1 μm, whereas the models assume a strictly uniform 1 μm diameter population in suspension. The 'Bubbicles' suspension scattering is consistent with predictions from the models, assuming gas volume fractions on the order of 10^{-2}. This volume fraction is not easy to verify independently, but is reasonable, given the surface morphology shown in Fig. 2(b) and the fact that the suspensions do not 'float' (as would be the case if the gas volume fraction exceeded 58%).

As mentioned in the introduction, the modeling assumed a uniform size distribution and a constant number density regardless of the volume fraction of gas [redacted] sized that only a small volume fraction of gas was [redacted] the scattering agent, assuming a constant number density equal to that for particles with no entrapped gas should adequately reflect the actual circumstances. The variation in the size distribution presents a number of additional issues in terms of possible resonance frequencies and scattering cross-sections. In the size range of interest (mean radius of 0.5–1 μm), as mentioned earlier, the larger scatterers would have to be comprised almost entirely of gas to consider resonance effects, a situation which physical observation of the agent in question discounts. In terms of the effect of scatterer size on the [redacted] of the radius, it should be remembered that the backscatter coefficient is determined by the number density of the scatterers, which is inversely proportional to at least the third power of the radius of the scatterers depending on spherical packing considerations. Since small volume fractions of gas produce such a significant change in the echogenicity of the scatterers, it would seem that the variation in differential scattering due to the distribution of volume fraction of gas values would be offset by the variation in number density due to the distribution of scatterer sizes. Further, it should be emphasized that the study was performed with a tone burst stimulus and provided a value for the backscatter coefficient at a [redacted] careful consideration of scatterer size variability. While [redacted] stance, it would tend to detract from the main focus of this study which was to evaluate the significant gain in scattering possible from solid Rayleigh type scattering [redacted] them. In fact, a more comprehensive study to precisely determine the effects of particle size variability and [redacted] modeling approach that has been presented here.

Important clinical implications may be derived from these results. In order to obtain a contrast agent that provides useful blood and liver reticulo-endothelial (RE) cell phases, we must ensure that a stabilized gas volume fraction on the order of 10% is carried by the particles. Blood and liver concentrations of IDE and 'Bubbicles' in the range of 2–3 mg cc^{-1} are achievable and non-toxic [11], therefore, the approach is promising.

Acknowledgement

This work was supported in part by NIH grant CA44732.

[redacted]

[1] R. Gramiak, P.M. Shah, Echocardiography of the aortic root, Investigative Radiology 3 (1968) 356.

[2] H. Feigenbaum, Echocardiography, 5th edn, Lea and Feibiger, Philadelphia, PA, 1994, pp. 119–121.

[3] D.L. Miller, Ultrasonic detection of resonant cavitation bubbles in a flow tube by the second-harmonic emissions, Ultrasonics September (1981) 217.

[4] T.G. Leighton, The Acoustic Bubble, Academic Press, London, 1994, pp. 67–72, 83–93.

[5] J.J. Bikerman, Physical Surfaces, Academic Press, New York, 1970, pp. 57–61.

[redacted]

[7] L. Crum, Acoustic cavitation, Notes for a short course given at Rochester Center for Biomedical Ultrasound, 1985.

[8] J. Ophir, K.J. Parker, Contrast agents in diagnostic ultrasound, Ultrasound in Medicine and Biology 15 (4) (1989) 319.

[9] H. Bleeker, K. Shung, J. Barnhart, On the application of ultrasonic contrast agents for blood flowmetry and assessment of cardiac perfusion, Journal Of Ultrasound in Medicine 9 (1990) 461.

[10] M.W. Keller, S.B. Feinstein, R.A. Briller, S.M. Powsner, Automated production and analysis of contrast agents, Journal of Ultrasound in Medicine 5 (1986) 493.

[11] M.R. Violante, R.B. Baggs, T. Tuthill, P. Dentinger, K.J. Parker, Particle stabilized bubbles for enhanced organ ultrasound [redacted] Ultrasound in Medicine and Biology 13 (9) (1987) 555.

[13] K.J. Parker, R.B. Baggs, R.M. Lerner, T.A. Tuthill, M.R. Violante, Ultrasound contrast for hepatic tumors using IDE particles, Investigative Radiology 25 (1990) 1135.

[14] M.R. Violante, K. Mare, H.W. Fischer, Biodistribution of a particulate hepatolienographic CT contrast agent: a study of iodi- [redacted] (1981) 40.

pam(Radiology) Tj 0 Tr4308 TDD 3 T6Tr -0.0ble 0.0344 Tw (1) Tj 0 Tr4308 TDD 3 T6Tr

[15] T.A. Tuthill, R.B. Baggs, M.R. Violante, K.J. Parker, Ultrasound properties of liver with and without particulate contrast agents, Ultrasound in Medicine and Biology 17 (3) (1991) 231.

[redacted] Hill, New York, 1968, pp. 356, 398–441.

[redacted] bles in water, Journal of the Acoustic Society of America 84 (3) (1988) 985.

[18] E.C. Everbach, Tissue composition determination via measurement of the acoustic nonlinearity parameter, Ph.D. Thesis, Yale University, 1989.

[19] K.A. Wear, M.R. Milunski, S.A. Wickline, J.E. Perez, B.E. Sobel, J.G. Miller, Contraction-related variation in frequency dependence of acoustic properties of canine myocardium, Journal of the Acoustic Society of America 86 (6) (1989) 2067.

[redacted] (1984) 913.

[21] M.F. Insana, E.L. Madsen, T.J. Hall, J.A. Zagzebski, Tests of the accuracy of a data reduction method for determination of acoustic backscatter coefficients, Journal of the Acoustic Society of America 79 (5) (1986) 1230.

[22] X. Chen, K.Q. Schwarz, K.J. Parker, Acoustic coupling from a [redacted] Journal of the Acoustic Society of America 95 (6) (1994) 3049.

[23] AIUM Standard Methods for Measuring Performance of Pulse-Echo Ultrasound Imaging Equipment, Rockville, MD, American Institute of Ultrasound in Medicine, 1991, p. 38.

[redacted] scattering cross sections of some human and animal tissues, Jour- [redacted]

[25] D.Y. Fei, K.K. Shung, Ultrasonic backscatter from mammalian tissues, Journal of the Acoustic Society of America 78 (3) (1985) 871.

[26] K.K. Shung, Y.W. Yuan, D.Y. Fei, Effect of flow disturbance on ultrasonic backscatter from blood, Journal of the Acoustic Society of America 75 (3) (1984) 1265.